SEMARAK ILMU PUBLISHING

Journal of Advanced Research in Fluid Mechanics and Thermal Sciences

Journal homepage:
https://semarakilmu.com.my/journals/index.php/fluid_mechanics_thermal_sciences/index
ISSN: 2289-7879

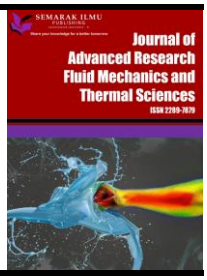

Determination of Thermal Conductivity Constant for Spray-Dried Mung Bean Protein Isolate using Series-Parallel "Block" Method and Central Composite Design

Zaida[1], Edy Suryadi[2], Adi Md. Sikin[3], Mohd Nizam Lani[4], Robi Andoyo[1,*]

[1] Department of Food Industrial Technology, Faculty of Agroindustrial Technology, Universitas Padjadjaran, Bandung, Indonesia
[2] Department of Agricultural Engineering and Bioprocess, Faculty of Agroindustrial Technology, Universitas Padjadjaran, Bandung, Indonesia
[3] Faculty of Applied Sciences, Universiti Teknologi MARA (UiTM), Shah Alam, Selangor, Malaysia
[4] Faculty of Fisheries and Food Science, Universiti Malaysia Terengganu, Kuala Nerus, Terengganu, Malaysia

ARTICLE INFO

Article history:
Received 3 November 2023
Received in revised form 25 January 2024
Accepted 5 February 2024
Available online 29 February 2024

Keywords:
Mung bean protein isolate; optimization; central composite design; series-parallel combination

ABSTRACT

The efficient production of mung bean protein isolate (MBPI) is essential for sustainable food processing, yet it is energy-intensive due to drying phase required to convert raw mung beans into a fine powder. This work was carried out to calculate the thermal conductivity constant ($\mathcal{k}$) of protein (A), moisture (B) and residual carbohydrate (C) of spray-dried MBPI. The protein slurry was prepared by dissolving MBPI in water at the ratio of 1:3, 1:4, and 1:5 prior to spray drying. The protein slurry was then spray dried at three different inflow temperatures of 140, 160, and 180 °C. A Series and Parallel Combination "Block" Model in tandem with a Central Composite Design (CCD) were selected to calculate the thermal conductivity constant of A, B and C. Eight arrangement components on A, B, and C component, measurements were derived from the initial three data points by utilizing the CCD method, in the preliminary study. By utilizing the series-parallel approach and statistical combination, there are a total of forty study arrangements. The thermal conductivity of MBPI with arrangements of A, B, and C (pABC); and a series of combinations of A and C in parallel to B (sAC pB) ranged from 0.1964-0.224 Wm^{-1} $°C^{-1}$, with R^2 = 98.73%-99.42%. Therefore, the energy requirement of spray drying process for MBPI could be predicted by the thermal properties of each component selected in the protein isolate.

1. Introduction

Mung beans are Mung beans are potentially a great source of plant-based protein with low amount of fat as compared to that from animal sources. It was reported that the protein and fat content of mung bean is ranged between 25–28% and 1–2%, respectively [1]. Protein isolate is a protein with the highest concentration and increased digestibility, which can be incorporated into various food products as food ingredient [2]. Drying is required to concentrate protein content from food sources. For example, spray drying yielded in 73.34%–82.81% protein in mung bean protein

* *Corresponding author.*
E-mail address: r.andoyo@unpad.ac.id

https://doi.org/10.37934/arfmts.114.2.155164

isolate (MBPI) in the current study. This is in accordance with Brishti *et al.,* [3], who reported that protein content of mung bean after drying was greater than 70%, though freeze drying resulted in greater amount of protein (86.15%) in MBPI.

Thermal conductivity (k) of MBPI is an important parameter in the determination of energy required for spray drying. Based on a study of Ravikanth *et al.,* [4], the k value of mung bean had a linear increase from 0.092 to 0.141 Wm^{-1} °C^{-1} when the moisture content increase. In wet conditions, the k value was increased from 9.9 to 18.3% when exposed to temperatures ranging from 10°C to 50°C [4]. The linear regression analysis of the natural logarithm of temperature against time yielded a gradient ranging from 0.465 to 1.595 at the temperature from 0 to 30°C.

The energy transfer rate is directly proportional to the thermal conductivity constant of the material and the temperature gradient established across its material thickness [5]. The energy is directly proportional to the coefficient of thermal conductivity during MBPI processing at constant temperature gradient. This current study was carried out to determine the thermal conductivity for each constituent component of MBPI. The k was multiplied by the constant factor (ki) with the proportion content of each constituent ingredient as described by Singh and Heldman [6] and Sahin and Sumnu [7]. The heat conductivity varies depending on the arrangement of the elements in series or parallel, as well as the statistical combinations of these components. The calculated value of k was then compared to the reference of the Virtual Experiment, and the findings were assessed [8].

In the current work, the components of MBPI, namely protein (A), water content (B), and carbohydrates (C) were considered as "block" solids. The limitation of this study was all components of MBPI were assumed as non-porous as the average pore size has a minimal impact on the effective thermal conductivity [9]. A limitation of this study is the assumption that all components of the MBPI are non-porous. This assumption is based on the rationale that the average pore size exerts a negligible impact on the effective thermal conductivity [9].

According to recent research by Bhattacharya [10] and seminal work by Box and Draper [11], the Central Composite Design (CCD) methodology, a well-known method in experimental design, offers numerous noteworthy advantages. The ability of CCD to effectively investigate and simulate complex response surfaces is one of its main advantages, particularly when interactions and quadratic effects are present. When it comes to response surface methods or optimizing experimental settings, this function is quite helpful. Moreover, in comparison to other design techniques, the systematic and thorough exploration of the experimental space is made possible by the organized approach of CCD. This in-depth investigation is essential for determining ideal circumstances and comprehending how different elements affect the response variable.

The effect of CCD on the properties of the data is another important factor. Because of the architecture, a large and distributed data set is guaranteed, making it easier to evaluate whether the correlations between the variables are linear or non-linear. A distribution of data points like this, which frequently includes axial, factorial, and centre points, improves the validity and robustness of the statistical models that are created. Because of its extensive coverage of the experimental region, CCD is especially useful in sectors where data processing validity and precision are crucial. This enables for more precise and dependable predictions.

Overall, the CCD technique greatly enhances the validity and dependability of data processing in experimental research due to its systematic approach and ability to produce widely distributed and well-dispersed data. Because of these characteristics, it is a recommended option in many scientific and technical applications where it is essential to comprehend the interaction and quadratic impacts of variables. Therefore, the objectives of the study were to determine the thermal conductivity constant for spray-dried MBPI using Series-Parallel “Block” Method and Central Composite Design.

2. Methodology

2.1 Materials

The production of MBPI was carried out by preparing the protein slurry at three dissolution ratios between protein isolate deposits and distilled water of 1:3, 1:4 and 1:5, prior to spray drying. The protein slurry was then dried at three different inlet temperatures of 140°C, 160°C, and 180°C using a mini spray dryer (B-290 Buchi) [12].

2.2 Method for Series and Parallel Combination "Block" Model

The preliminary experimental results indicated that the MBPI aggregation yielded the three component of protein (A), water content (B), and residual carbohydrate (C). As shown in Table 1, the protein and moisture content of MBPI ranged between 73.34-82.81% and 3.45-8.65%, respectively. Thus, the remaining portion consists of carbohydrates (C). By setting up the three parts in a series-parallel pattern and using statistical combinations shown in Eq. (1), eight ABC combinations were obtained with heat flow direction as shown in Figure 1.

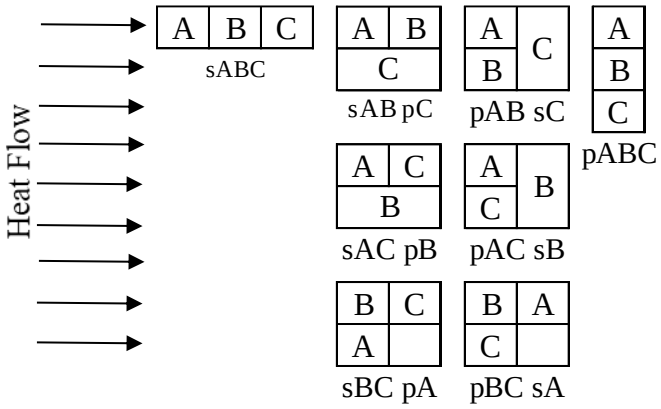

Fig. 1. The spray drying of MBPI was carried out by eight permutations of protein (A), water content (B), and residual carbohydrate (C)

Applying the formula by Kaloyerou [13] to a combination with three ingredients (A, B, and C), we have n = 3 and p = 1, 2, 3.

$$C_p^n = \frac{n!}{(n-p)!p!} \tag{1}$$

Central Composite Design (CCD) was used to investigate three independent variables; the composition of protein (A), water content (B) and carbohydrate (C) in MBPI at five different levels (-α, -1, 0, 1, +α) as shown in Table 1. The concentration of component A, B, and C was connected to the thermal conductivity constant k as a function of time from Eq. (5), Eq. (6) and Eq. (7), respectively. The binomial combination of the series-parallel connection yielded eight values for thermal conductivity constant of each component as shown in Figure 1.

Table 1
Composition of protein, water content and carbohydrate in MBPI coded as A, B and C, respectively

Component	Concentration				
	-α	-1	0	+1	+α
Protein Isolate (A)	0.6955	0.7334	0.7890	0.8281	0.8548
Water Content (B)	0.0205	0.0345	0.0550	0.0737	0.0865
Carbohydrate (C)	0.2840	0.2321	0.1560	0.0982	0.0588

Prior to this work, the concentration of each component A, B and C was obtained experimentally and coded as $-1, 0, 1$ [10, 14]. On the other hand, the concentration determined by CCD was coded as $-\alpha$ and $+\alpha$ [14]. For each component A, B, and C, the minimum, average and maximum concentration of each component was denoted as -1, 0 and +1. As shown in Table 1, the value of α was defined as distance of each axial point from the center. α is known as rotatability and expressed in Eq. (2) [10,15,16].

$$\alpha = (2^k)^{0.25} \tag{2}$$

The number of predictor factors was presented as variable k which in this case is equal to 3. The concentration data, represented as $-\alpha$ and $+\alpha$ were determined by applying the rotatability value (α) to the lowest and highest coded levels, denoted as K_{-} and K_{+} , respectively.

$$\mathrm{K}_{-} = -\alpha\,(\mathrm{L}) + \mathrm{C} \tag{3}$$

$$\mathrm{K}_{+} = \alpha(\mathrm{L}) + \mathrm{C} \tag{4}$$

L = delta value in codes 1 and 0;
C = center point value.

The thermal conductivity of each component in MBPI was empirically expressed in Eq. (5) to Eq. (7). It is as a function of temperature was shown in Eq. (5) to Eq. (7) [7].

$$k_{protein} = 0.17881 + 1.1958 \times 10^{-3}T - 2.7178 \times 10^{-6}T^2 \tag{5}$$

$$k_{water} = 0.57109 + 1.7625 \times 10^{-3}T - 6.7036 \times 10^{-6}T^2 \tag{6}$$

$$k_{carbohydrate} = 0.20141 + 1.3874 \times 10^{-3}T - 4.3312 \times 10^{-6}T^2 \tag{7}$$

It is the sum of each element's productivities as a function of material temperature; Eq. (4) to Eq. (5); with the proportion concentration of each constituent. MBPI with three components A, B, and C for series-parallel arrangement and derived eight arrangements as shown in Figure 1, from the statistical combination formula expressed in Eq. (1) [7].

The thermal conductivity (k) was determined by arranging the three components of MBPI in a series (k_{se}) and parallel (k_{pa}) configuration, which is perpendicular to the direction of heat flow [6,7].

$$\frac{1}{k_{se}} = \frac{X_{pro}^{v}}{k_{pro}} + \frac{X_{water}^{v}}{k_{water}} + \frac{X_{carb}^{v}}{k_{Carb}} \tag{8}$$

$$\hbar_{pa} = \hbar_{pro} X^{v}_{pro} + \hbar_{water} X^{v}_{water} + \hbar_{Carb} X^{v}_{carb} \quad (9)$$

$$X_i^v = \frac{1}{\left(\sum_{i=1}^{n} \frac{X_i^v}{\rho_i}\right)} \left(\frac{X_i^w}{\rho_i}\right) \quad (10)$$

Note:
X_i^v =volume fraction of the i[th] constituent.
X_i^w =mass fraction of the ith constituent.
ρ_i = density of the i[th] constituent (kg m^{-3}).

3. Results

In this current work, the treatment codes representing the selected composition of MBPI were generated resulting in five concentration level and eight potential object arrangements, for a total of forty arrangements used. The five concentration of each component was coded as -α, -1, 0, +1, +α giving substances identified as MBPI-α, MBPI-1, MBPI-0 MBPI+1 MBPI+α, respectively. The arrangement of A, B, and C in series and parallel was represented as sABC and pABC, respectively. For example, the notation of sAB pC was used to represent the combination of series A and B in parallel with C.

Out of the 40 arrangements, 9 graphs primarily 4 pABC, 4 sAC pB, and 1 sAB pC were found to match with the VE data requirements as shown in Figure 1. On the contrary, thirty more combinations fall short of the specifications with VE reference data. As shown in Table 2, the graph exhibiting the lowest thermal constant value is pABC-α, with a value of $\hbar$=0.1667 $\mathrm{Wm^{-1}{}^{\circ}C^{-1}}$), while the highest value is sAC pB+1, $\hbar$=0.2648 $\mathrm{Wm^{-1}{}^{\circ}C^{-1}}$ in the series-parallel arrangement of thermal conductivity.

3.1 MBPI-α

As shown in Figure 2, the VE referenced value of $\hbar$ ranged between 0.1692 and 0.2194 $\mathrm{Wm^{-1}{}^{\circ}C^{-1}}$, with an average of 0.1951 ± 0.0150 $\mathrm{Wm^{-1}{}^{\circ}C^{-1}}$. At MBPI-$\alpha$, the range of $\hbar$ was between 0.1729–0.2252 $\mathrm{Wm^{-1}{}^{\circ}C^{-1}}$with an average value of 0.1964-0.0157 $\mathrm{Wm^{-1}{}^{\circ}C^{-1}}$ for pABC and sAC pB, respectively. A similar gradient of 0.0013 for a linear curve of VE, sAC pB and pABC with a coefficient R^2 ranging from 99.92% - 99.93%.

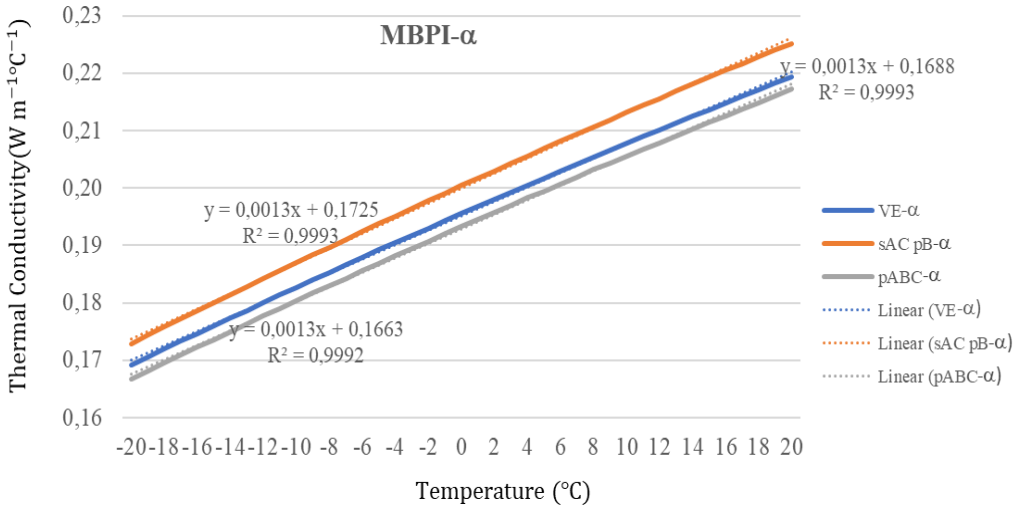

Fig. 2. Graphs comparing thermal conductivity vs. temperature for MBPI-α and VE-α

3.2 MBPI-1

As shown in Figure 3, the VE referenced value of $\hbar$ ranged between 0.1711-0.2355 $\mathrm{Wm^{-1}{}^{\circ}C^{-1}}$, with an average of = 0.2014 ± 0.0150 $\mathrm{Wm^{-1}{}^{\circ}C^{-1}}$. At MBPI-1, the range of $\hbar$ was between 0.1667–0.2252 $\mathrm{Wm^{-1}{}^{\circ}C^{-1}}$ with an average value of 0.2034-0.0167 0.1964-0.0157 $\mathrm{Wm^{-1}{}^{\circ}C^{-1}}$ for pABC and sAC pB, respectively. A similar gradient of 0.0013 for a linear curve of VE, sAC pB and pABC with a coefficient R^2 of 99.93%.

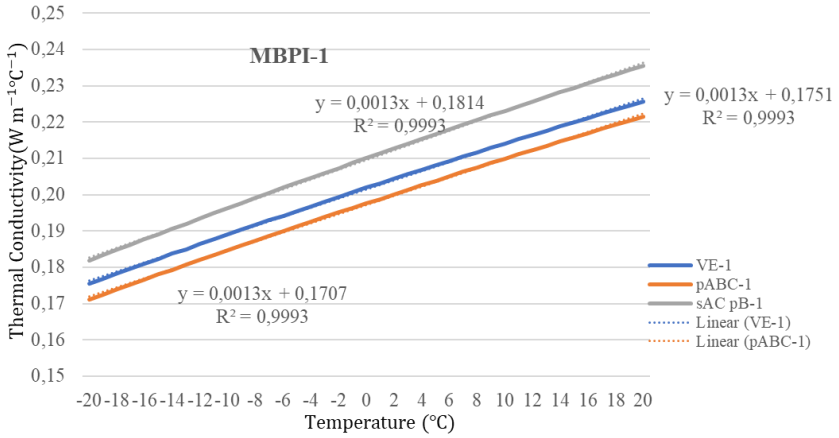

Fig. 3. Graphs comparing thermal conductivity vs. temperature for MBPI-1 and VE-1

3.3 MBPI-0

The plot representing the effect of temperature on thermal conductivity between MBPI-0 and VE-0 was discussed based on its linearity and shown in Figure 4. The $\hbar$ values of 0.2285-0.4562 $\mathrm{Wm^{-1}{}^{\circ}C^{-1}}$ and 0.2285-0.2530 $\mathrm{Wm^{-1}{}^{\circ}C^{-1}}$ were obtained for the non-linear and linear component of VE-0 reference data, respectively. The average value of $\hbar$ was 0.3316 $\pm$ 0.1014 $\mathrm{Wm^{-1}{}^{\circ}C^{-1}}$. Furthermore, a linear trend with R^2 = 99.92% was differed from that of non-linear portion of the data distribution, which exhibits a polynomial linear trend of R^2 = 74.9%. At MBPI-0, a range of $\hbar$ = 0.1950-0.2519 $\mathrm{Wm^{-1}{}^{\circ}C^{-1}}$ was determined for the arrangement of sAC pB. The mean $\hbar$ was 0.2244 $\pm$ 0.1704 $\mathrm{Wm^{-1}{}^{\circ}C^{-1}}$. The gradient of 0.0012-0.0014 was calculated with the coefficient R^2 ranging from 99.92% to 99.99%. Precise data were presented by nearly congruent lines in linear segment of the plots for both MBPI-0 and VE-0 as shown in Figure 4.

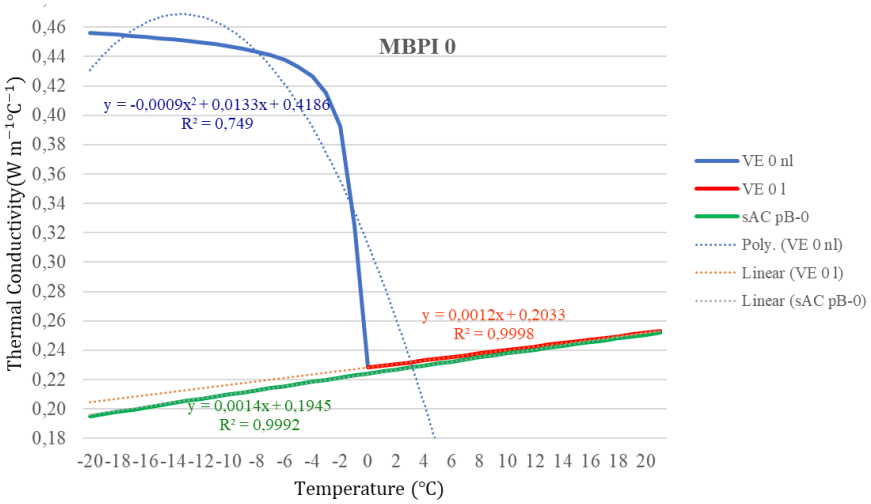

Fig. 4. Graphs comparing thermal conductivity vs. temperature for MBPI-0 and VE-0

3.4 MBPI+1

As shown in Figure 5, the plot representing the effect of temperature on thermal conductivity between MBPI+1 and VE-+1 was discussed based on its linearity. The $\hbar$ values of 0.2097- 0.3274 $Wm^{-1}°C^{-1}$ and 0.2100-0.2427 $Wm^{-1}°C^{-1}$ were obtained for the non-linear and linear component of VE+1reference data, respectively. The average value of $\hbar$ was 0.2454 $\pm$ 0.0359 $Wm^{-1}°C^{-1}$. Furthermore, a linear trend with R^2 = 99.96% was differed from that of non-linear portion of the data distribution, which exhibits a polynomial linear trend of R^2 = 99.66%. At MBPI+1, a range of $\hbar$ = 0.1950-0.2519 $Wm^{-1}°C^{-1}$ was determined for the arrangement of pABC and sAB pC. The mean $\hbar$ was 0.2201 $\pm$ 0.197 $Wm^{-1}°C^{-1}$. The gradient of 0.0012 and 0.0014 was calculated with the coefficient R^2 ranging from 99.92% to 99.99%. Precise data were presented by nearly congruent lines in linear segment of the plots for both MBPI+1 and VE+1-as shown in Figure 5.

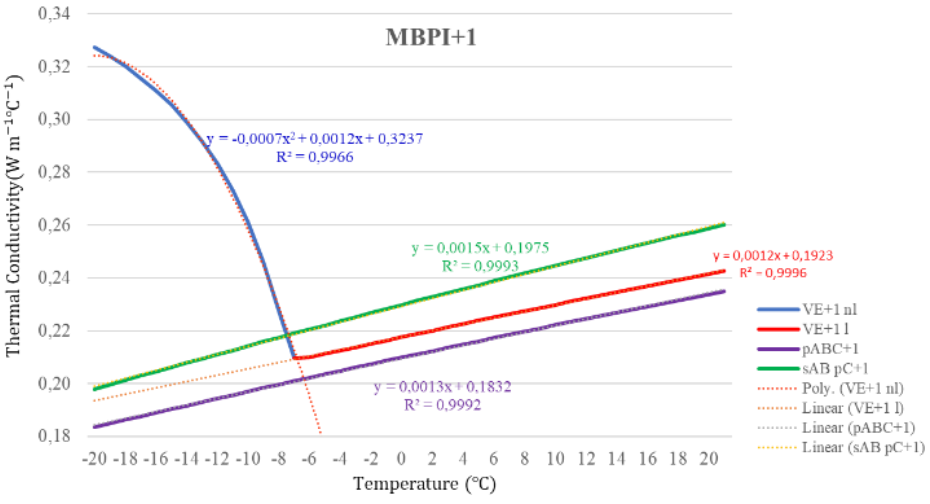

Fig. 5. Graphs comparing thermal conductivity vs. temperature for MBPI+1 and VE+1

3.5 MBPI+α

The plot representing the effect of temperature on thermal conductivity between MBPI+α and VE+α was discussed based on its linearity. The $\hbar$ values of 0.2196-0.3916 $\mathrm{Wm^{-1}{}^{\circ}C^{-1}}$ and 0.2205-0.2481 $\mathrm{Wm^{-1}{}^{\circ}C^{-1}}$ were obtained for the non-linear and linear component of VE+α reference data, respectively. The average value of $\hbar$ was 0.2793 $\pm$ 0.0640 $\mathrm{Wm^{-1}{}^{\circ}C^{-1}}$. Furthermore, a linear trend with R^2 = 99.92% was differed from that of non-linear portion of the data distribution, which exhibits a polynomial linear trend of R^2 = 97.71%. At MBPI+α, a range of $\hbar$ = 0.1849-0.2428 0.1950-0.2519 $\mathrm{Wm^{-1}{}^{\circ}C^{-1}}$ was determined for the arrangement of pABC and sAB pC. The mean $\hbar$ was 0.2154 $\pm$ 0.0163 $\mathrm{Wm^{-1}{}^{\circ}C^{-1}}$. The gradient of 0.0012-0.0014 was calculated with the coefficient R^2 ranging from 99.93% and 99.98%. Precise data were presented by nearly congruent lines in linear segment of the plots for both MBPI+α and VE+α as shown in Figure 6.

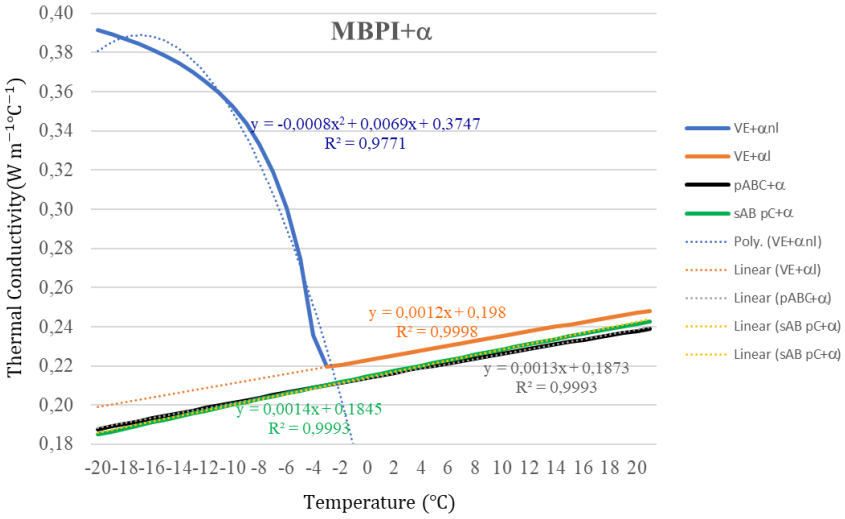

Fig. 6. Graphs comparing thermal conductivity vs. temperature for MBPI+α and VE+α

4. Discussion

The thermal conductivity of ice is approximately four times greater than that of liquid water [6]. Based on the outcomes derived from series-parallel computations (Figure 2 and Figure 3), CCD treatment codes, and statistical combination permutations, it has been observed that a water content below 5% does not significantly impact the properties of MBPI and preserves its linear behaviour. In this study, the water content in the MBPI exceeded 5%, leading to the nonlinearity observed in Figure 4, Figure 5, and Figure 6. Notably, the most significant increase in thermal conductivity was identified at temperatures approximately 10°C lower than the standard freezing point [6].

The calculated values of thermal conductivity (k) for MBPI, ranging from MBPI-α to MBPI+α, should align with the established VE (Virtual Experiments) reference values. Consequently, accurately determining the coefficient of determination for the thermal conductivity of each MBPI component is crucial. Table 2 presents the relationship between the thermal conductivity of MBPI and the percentage composition of each of its components (A, B and C) obtained from this study.

Table 2
Thermal Conductivity versus MBPI Component

Thermal conductivity ($Wm^{-1}°C^{-1}$)	% Protein (A)	% Water content (B)	% Carbohydrate (C)
0.1964	69.55	2.05	28.40
0.2034	73.34	3.45	23.21
0.2244	78.90	5.50	15.60
0.2201	82.81	7.37	9.82
0.2145	85.48	8.65	5.8

As shown in Figure 7, the level of closeness or coefficient of determination (R^2) for protein, water content and carbohydrate in MBPI was 98.73%, 99.42% and 99.01%, respectively. These values signify the strength of correlation between the variables of the regression equation and the data presented in Table 2. The process requires the selection of graph data that exhibits a strong correlation with the VE data. This can be accomplished by averaging the data from two highly correlating graphs out of a set of eight graphs, or by analyzing more than two graphs. However, the latter approach typically results in an R^2 value below 90%.

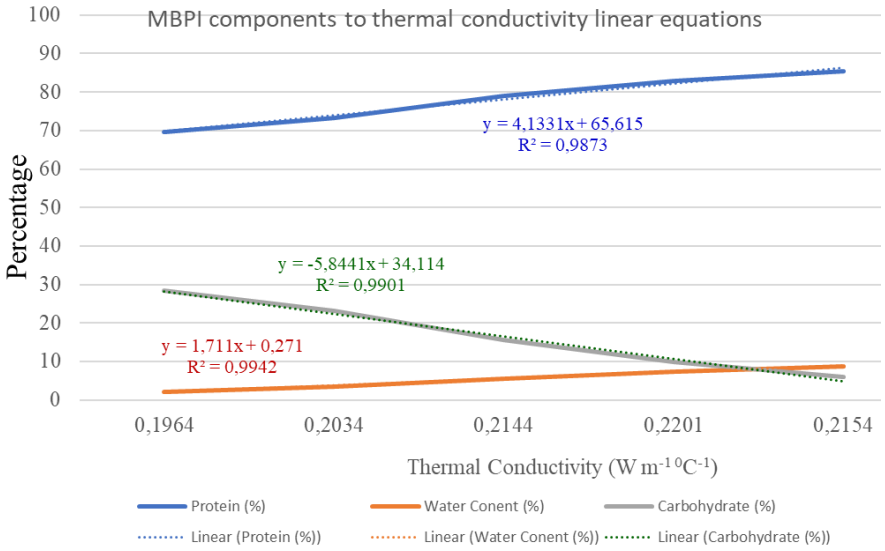

Fig. 7. MBPI Components to Thermal Conductivity k Linear Equation

5. Conclusion

Overall, a greater quantity and variation of data was detected when analysing the concentration of each component selected in MBPI. The contents of protein, water and carbohydrate were taken into account to obtain the conductivity constant (k) of the MBPI. Preliminary research was conducted using three datasets, representing the lowest (code -1), average (code 0), and highest (code +1) values for the concentration of each component in MBPI. The treatment codes, code -α and code +α, yield five key data points on the composition of MBPI concentration. The codes MBPI-α, MBPI-1, MBPI-0, MBPI+1, and MBPI+α represent these data points.

In this study, every composition of protein, water and carbohydrate in MBPI was used in the permutations and statistical combinations, leading to a total of eight potential parallel series arrangements, and a total of 40 distinct series and parallel arrangements. Out of these 40 arrangements in parallel series, nine arrangements were found to align with the specifications from

the virtual experiment (VE) during our investigation of the thermal conductivity (k) of MBPI. Particularly, there were 4 of pABC and 5 sAC pB could be arranged.

The nine arrangements were categorized into five groups based on their concentration, each having an average value of thermal conductivity. A k-value of 0.1964 and 0.2034 Wm^{-1} $^{o}C^{-1}$ was obtained with the arrangement of pABC for MBPI-α. The k-value of 0.2201 and 0.2145 Wm^{-1} $^{o}C^{-1}$ was determined by pABC and sAC for MBPI+1 and MBPI+α, respectively. Similarly, the k-value of 0.2034 and 0.2244 was obtained with the same arrangement of sAC pB for MBPI-1 and MBPI-0, respectively. For future study, we would like to apply the findings to real-world scenarios or industrial applications where MBPI is used, to validate the laboratory findings and explore practical challenges and solutions.

Acknowledgement
The financial support from Universitas Padjadjaran is gratefully acknowledged. The authors are grateful to Directorate of Research, Community Service, and Innovation as well as Faculty of Agricultural Industrial Technology, Universitas Padjadjaran for providing the lab facilities and valuable suggestions on modelling.

References

[1] Khaket, Tejinder Pal, Suman Dhanda, Druksakshi Jodha, and Jasbir Singh. "Purification and biochemical characterization of dipeptidyl peptidase-II (DPP7) homologue from germinated Vigna radiata seeds." *Bioorganic Chemistry* 63 (2015): 132-141. https://doi.org/10.1016/j.bioorg.2015.10.004
[2] Garba, Umar, and Sawinder Kaur. "Protein isolates: Production, functional properties and application." *International Journal of Current Research and Review* 6, no. 3 (2014): 35.
[3] Brishti, Fatema Hossain, Shyan Yea Chay, Kharidah Muhammad, Mohammad Rashedi Ismail-Fitry, Mohammad Zarei, Sivakumaran Karthikeyan, and Nazamid Saari. "Effects of drying techniques on the physicochemical, functional, thermal, structural and rheological properties of mung bean (Vigna radiata) protein isolate powder." *Food Research International* 138 (2020): 109783. https://doi.org/10.1016/j.foodres.2020.109783
[4] Ravikanth, L., D. S. Jayas, K. Alagusundaram, and V. Chelladurai. "Measurement of thermal properties of mung bean (Vigna radiata)." *Transactions of the ASABE* 55, no. 6 (2012): 2245-2250. https://doi.org/10.13031/2013.42481
[5] Paraschiv, Lizica Simona, Nicoleta Acomi, Alexandru Serban, and Spiru Paraschiv. "A web application for analysis of heat transfer through building walls and calculation of optimal insulation thickness." *Energy Reports* 6 (2020): 343-353. https://doi.org/10.1016/j.egyr.2020.08.055
[6] Singh, R. Paul, and Dennis R. Heldman. *Introduction to food engineering*. Academic Press, 2008.
[7] Sahin, Serpil, and Servet Gülüm Sumnu. *Physical properties of foods*. Springer Science & Business Media, 2006.
[8] Singh, R. Paul. "Importance of thermophysical properties." *rpaulsingh*, 2023. http://www.rpaulsingh.com/learning/virtual/experiments/physproperties/index.html.
[9] Carson, James K., Simon J. Lovatt, David J. Tanner, and Andrew C. Cleland. "Experimental measurements of the effective thermal conductivity of a pseudo-porous food analogue over a range of porosities and mean pore sizes." *Journal of Food Engineering* 63, no. 1 (2004): 87-95. https://doi.org/10.1016/S0260-8774(03)00286-3
[10] Bhattacharya, Sankha. "Central composite design for response surface methodology and its application in pharmacy." In *Response Surface Methodology in Engineering Science*. IntechOpen, 2021. https://doi.org/10.5772/intechopen.95835
[11] Box, George E. P., and Norman R. Draper. Empirical model-building and response surfaces. John Wiley & Sons, 1987.
[12] Haque, M. Amdadul, and Benu Adhikari. "Drying and denaturation of proteins in spray drying process." *Handbook of Industrial Drying* 33, no. 10 (2015): 971-985. https://doi.org/10.1080/07373937.2015.1023311
[13] Kaloyerou, Panayiotis Nicos. *Basic Concepts of Data and Error Analysis*. Cham: Springer International Publishing, 2018. https://doi.org/10.1007/978-3-319-95876-7
[14] Wu, C. F. Jeff, and Michael S. Hamada. Experiments: planning, analysis, and optimization. John Wiley & Sons, 2009.
[15] Khuri, Andre I., and John A. Cornell. *Response surfaces: designs and analyses*. Routledge, 2018. https://doi.org/10.1201/9780203740774
[16] Myers, Raymond H., Douglas C. Montgomery, and Christine M. Anderson-Cook. *Response surface methodology: process and product optimization using designed experiments*. John Wiley & Sons, 2009.